Human Molecular Genetics, 2012, Vol. 21, No. 14 **3193–3204**
doi:10.1093/hmg/dds144
Advance Access published on April 14, 2012

Impaired calcium calmodulin kinase signaling and muscle adaptation response in the absence of calpain 3

I. Kramerova[1], E. Kudryashova[1,†], N. Ermolova[1], A. Saenz[2,4], O. Jaka[2,4], A. López de Munain[2,3,4] and M.J. Spencer[1,*]

[1]Department of Neurology, David Geffen School of Medicine, University of California, Los Angeles, CA 90095, USA, [2]Neuroscience Area, Biodonostia Institute and [3]Department of Neurology, Hospital Universitario Donostia, 20014 San Sebastián, Spain and [4]CIBERNED, Centro de Investigaciones Biomédicas en Red sobre Enfermedades Neurodegenerativas, Institute Carlos III, Ministry of Science and Innovation, Spain

Received January 27, 2012; Revised March 14, 2012; Accepted April 9, 2012

Mutations in the non-lysosomal, cysteine protease calpain 3 (CAPN3) result in the disease limb girdle muscular dystrophy type 2A (LGMD2A). CAPN3 is localized to several subcellular compartments, including triads, where it plays a structural, rather than a proteolytic, role. In the absence of CAPN3, several triad components are reduced, including the major Ca^{2+} release channel, ryanodine receptor (RyR). Furthermore, Ca^{2+} release upon excitation is impaired in the absence of CAPN3. In the present study, we show that Ca-calmodulin protein kinase II (CaMKII) signaling is compromised in CAPN3 knockout (C3KO) mice. The CaMK pathway has been previously implicated in promoting the slow skeletal muscle phenotype. As expected, the decrease in CaMKII signaling that was observed in the absence of CAPN3 is associated with a reduction in the slow versus fast muscle fiber phenotype. We show that muscles of WT mice subjected to exercise training activate the CaMKII signaling pathway and increase expression of the slow form of myosin; however, muscles of C3KO mice do not exhibit these adaptive changes to exercise. These data strongly suggest that skeletal muscle's adaptive response to functional demand is compromised in the absence of CAPN3. In agreement with our mouse studies, RyR levels were also decreased in biopsies from LGMD2A patients. Moreover, we observed a preferential pathological involvement of slow fibers in LGMD2A biopsies. Thus, impaired CaMKII signaling and, as a result, a weakened muscle adaptation response identify a novel mechanism that may underlie LGMD2A and suggest a pharmacological target that should be explored for therapy.

INTRODUCTION

Limb girdle muscular dystrophy type 2A (LGMD2A) is one of the most frequently occurring forms of recessive LGMDs, which are diseases characterized by the primary involvement of scapular and pelvic muscles that demonstrate progressive muscle weakness. LGMD2A results from mutations in the gene encoding calpain 3 (CAPN3), a non-lysosomal Ca^{2+}-dependent cysteine protease (1,2). More than 400 different pathogenic *CAPN3* gene mutations have been identified to date, the majority of which represent non-synonymous amino acid substitutions (Leiden Molecular Dystrophy database/*capn3*). Interestingly, there is no apparent mutational hot spot in the *CAPN3* gene, but rather the mutations have a widespread distribution along the entire length of the gene (3). The distribution of many of these mutations, far from the active site, suggests that some of these mutations spare proper proteolytic activity of *CAPN3*. This observation is supported by biochemical studies in which one-third of 79 LGMD2A biopsies analyzed exhibited a near-normal level of CAPN3 proteolytic activity (4). Thus, these data suggest that CAPN3 plays both structural and proteolytic roles.

*To whom correspondence should be addressed at: 635 Charles Young Drive South, NRB Room 401, Los Angeles, CA 90095, USA. Tel: +1 3107945225; Fax: +1 3102061998; Email: mspencer@mednet.ucla.edu
†Present address: Department of Biochemistry, Ohio State University, Columbus, OH 43210, USA.

Several features distinguish CAPN3 from the better studied isoforms called CAPNs1 and 2, which are the ubiquitously expressed typical calpains. First, CAPN3 has three unique insertion sequences called NS, IS1 and IS2, which are not found in any other member of the calpain family (5). Second, although CAPN1 and 2 require association with a regulatory subunit for their activation, CAPN3 is activated through several steps of autolytic cleavage in the NS and IS1 domains, located at the N-terminus and the protease domain, respectively (6,7). The IS1 cleavage splits the protease domain into two fragments, which stay non-covalently associated with each other to enable proteolytic activity (6). These data obtained primarily *in vitro* suggest that the only proteolytically active configuration for CAPN3 consists of two autolytically derived fragments that are associated with each other. Neither the full-length 94 kDa form (readily detectable in extracts from skeletal muscles) nor each of the autolytic fragments alone possesses proteolytic activity; however, it is possible that these individual fragments may serve other distinct cellular roles.

CAPN3 resides in several different cellular compartments that include the myofibrillar, cytosolic and membrane fractions. At each of its cellular locations, it is likely that CAPN3 acts on different substrates and serves a multitude of roles. At least one fraction of the membrane-associated pool of CAPN3 places it at muscle triads in mice (8). Triads are specialized membranous structures in skeletal muscles, where the T tubules and sarcoplasmic reticulum (SR) interact to induce Ca^{2+} release from the SR in response to neural excitation (9). Sharply increased intracellular Ca^{2+} triggers muscle contraction, thus synchronizing neural excitation and cross-bridge activation, a process called excitation–contraction coupling. Our previous studies have shown that CAPN3 plays a structural role in the maintenance of a protein complex at the triad (8). In particular, CAPN3 interacts with the ryanodine receptor (RyR), a multisubunit protein that comprises the Ca^{2+} release channel, and levels of RyR are significantly reduced in the absence of CAPN3. Accompanying the reductions in RyR concentration is a significant decrease in Ca^{2+} release upon activation in isolated muscle fibers (8). Thus, CAPN3 is essential for sustaining the integrity of the triad and in its absence, impaired Ca^{2+} transport ensues. The data linking CAPN3 to the triad complex and the regulation of Ca^{2+} release were subsequently validated by Dayanithi *et al.* (10), who demonstrated a reduction in caffeine stimulated Ca^{2+} release in primary myotubes isolated from CAPN3 knockout (C3KO) muscles. In addition, CAPN3's association with triad SR components, as well as the structural role of CAPN3 in this complex, was corroborated in studies of knock-in mice that express only the proteolytically inactive mutant of CAPN3 (C129S) (11). These data, taken together, suggest that impairment of Ca^{2+} transport may be an underlying pathogenic feature of calpainopathy.

Fluctuations in intracellular Ca^{2+} normally occur during increased muscle activity and these associated elevations in intracellular Ca^{2+} can activate Ca^{2+}-mediated signaling pathways. Two such pathways operate via Ca^{2+}-calmodulin binding: the calcineurin (Cn)/NFAT pathway and the Ca^{2+}--calmodulin-dependent protein kinase (CaMK) pathway. Both pathways regulate gene expression in cardiac and skeletal muscle, leading to hypertrophic growth and promotion of the slow versus fast fiber phenotype in response to various types and levels of muscle activity (reviewed in 12 and 13; Figure 1). Ca^{2+}-calmodulin-dependent activation of Cn (a phosphatase) leads to the dephosphorylation of NFAT (nuclear factor of activated T cells), allowing its translocation to the nucleus, where it acts as a transcriptional co-activator to induce expression of downstream genes. Activated CaMK (a kinase), on the other hand, acts through the phosphorylation of class II histone deacetylases (HDACs). Dephosphorylated HDACs reside primarily in the nucleus, where they bind to and repress transcription factors such as MEF2 (myocyte enhancer factor) as well as regulate chromatin condensation. When phosphorylated by Ca-calmodulin protein kinase II (CaMKII), HDACs are translocated out of the nucleus by 14-3-3 chaperone proteins, thereby relieving the repression by HDACs and allowing MEF2-dependent transcriptional activation (12,13).

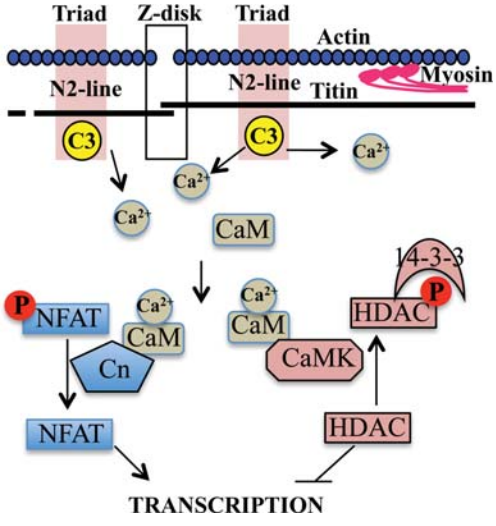

Figure 1. Schematic representation of two Ca^{2+}-mediated signaling pathways that have been shown to modulate muscle phenotype. One pathway (blue) is Cn-NFAT, whereas the second (pink) is CaMK—both are activated by CaM binding. Cn phosphatase acts on NFAT transcription factors, which activate transcription when dephosphorylated. CaMKs act on class II HDACs, which are transcriptional repressors when in the non-phosphorylated state. Phosphorylated HDACs bind adaptor proteins of the14-3-3 family, translocating them out of the nucleus, which releases repression of MEF2-regulated transcription.

Since our previous studies demonstrated that Ca^{2+} release upon activation was significantly reduced in C3KO muscles (8), we hypothesized that Ca^{2+}-mediated signaling may be impaired as a consequence. Inadequate activation of these pathways could potentially lead to an insufficient ability of muscle to adapt to changes in functional demands. In this investigation, we seek to find experimental support for this hypothesis by looking at various components of Ca^{2+}-mediated signaling pathways as well as downstream effects of impaired signaling on muscle adaptation in C3KO muscles and LGMD2A biopsies. We found that the CaMKII signaling is specifically reduced in the absence of CAPN3, leading to a decrease in the slow versus fast myofiber phenotype. This signaling was impaired both at rest and in response to physical exercise in C3KO mice. Furthermore, we examined LGMD2A biopsies and observed that RyR levels were

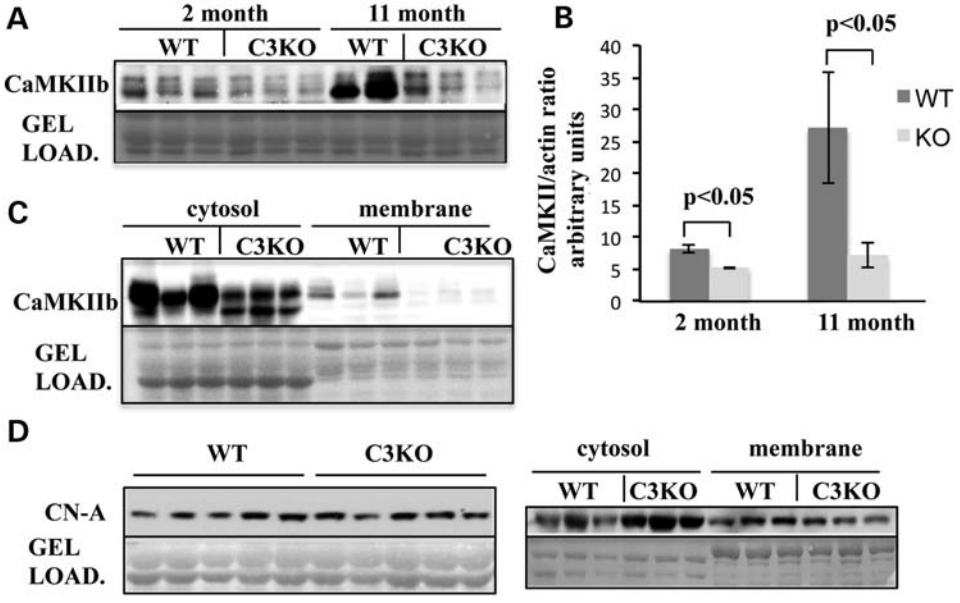

Figure 2. CaMKII expression is specifically blunted in C3KO muscles. (**A**) Western blot analysis of CaMKII content in whole-muscle extracts from young (2 month) and old (11 month) solei shows decreased CaMKII in C3KO muscles, and a lack of increased CaMKII with age. (**B**) Quantitative analysis of the blot demonstrating the densitometric value of CaMKII normalized for loading by densitometric assessment of actin in the same samples. Vertical bars represent standard error. (**C**) Western blot analysis of CaMKII in cytosol and membrane fractions from the diaphragm muscle shows that, in both fractions, CaMKII is decreased in C3KO muscles. CaMKII quantitation was done by summing the signals from both bands. (**D**) Western blot analysis of Cn in whole-muscle extracts from the soleus muscle (left panel) or fractions from the diaphragm muscle (right panel) from WT and C3KO mice. For all blots, loading controls are shown below the immunoblot.

decreased in the absence of CAPN3 protein, similar to that observed in C3KO mice. These same biopsies showed a corresponding, preferential involvement of slow-twitch fibers. Thus, impaired Ca^{2+}-mediated signaling and, as a result, weakened muscle adaptation represent a novel pathogenic mechanism that likely operates in CAPN3-deficient muscles.

RESULTS

CaMKII-mediated signaling is blunted in C3KO muscles

Elevated intracellular Ca^{2+} triggers the activation of several signaling pathways operating through binding to Ca^{2+}-calmodulin. In particular, the Cn-mediated and the CaMK-mediated pathways are activated in this manner, which allows for tight coupling between muscle activity and gene expression (Fig. 1). To investigate whether these pathways are altered due to the reduced Ca^{2+} that occurs in the absence of CAPN3, we first analyzed the levels of Cn and CaMKII in extracts from C3KO and wild-type (WT) muscles. Previously, we noticed that several triad-associated proteins were reduced in C3KO muscles, including CaMKII, RyR and triad-associated aldolase A (8). To determine whether these changes occurred more generally and were not only limited to the fraction of CaMKII that was triad-associated, we compared CaMKII in additional fractions from C3KO and WT muscles (Fig. 2A–C). Although CaMKII appeared to be enriched in the cytosolic versus the membrane fraction of both genotypes, CaMKII was significantly decreased in both fractions isolated from C3KO compared with WT muscles. In addition, we found that CaMKII is greatly elevated with aging (11 versus 2 months) and that C3KO mice fail to undergo similar elevations with aging (Fig. 2A and B). Cn levels were also examined and were not found to be decreased in whole-muscle extracts, nor in cellular fractions isolated from C3KO mice (Fig. 2D). Moreover, the concentration of Cn was higher in the cytosolic fraction from C3KO muscles, possibly as a compensatory mechanism for the reduction in CaMKII. Therefore, the absence of CAPN3 resulted in a specific reduction of CaMK-mediated signaling in C3KO muscles.

Following the binding of Ca^{2+}-calmodulin to CaMK II, it autophosphorylates and becomes constitutively active (14,15). We used an antibody that specifically recognizes activated CaMKII (alpha subunit phosphorylated at Thr286) to examine the concentration of activated CaMKII in C3KO muscle extracts. This analysis revealed that activated (P-Thr286) CaMKII is greatly reduced in both the cytosolic and membrane fractions of C3KO muscles, likely due to reductions in total CaMKII (Fig. 3A). Furthermore, since activated CaMKIIs phosphorylate class II HDACs and cause their translocation out of the nucleus resulting in the release of transcriptional repression (Fig. 1), we examined the level of nuclear HDAC in purified nuclear extracts from C3KO and WT muscles. Based on studies by Potthoff *et al.* (16), HDAC7 is greatly reduced in skeletal muscles of mice overexpressing CaMK, so this HDAC was focused upon for this investigation. Staining of cytosolic and nuclear extracts from C3KO and WT muscles revealed that although HDAC7 was slightly decreased in the cytosolic fraction of C3KO muscles, it accumulated in the nuclear fraction (Fig. 3B).

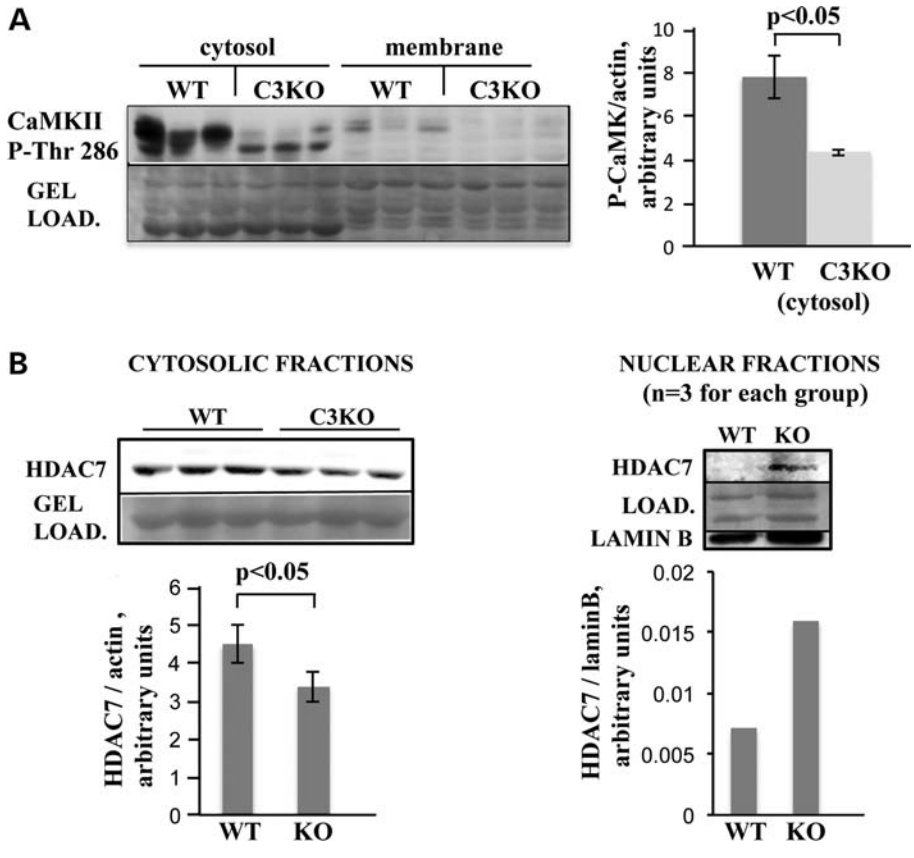

Figure 3. CaMKII activation is impaired in C3KO muscles. (**A**) Western blot analysis using an antibody against P-Thr286 on CaMK, which represents the autophosphorylated, activated CaMKII. The data show a reduction of P-Thr 286 CaMKII in both cytosol and membrane fractions from C3KO diaphragms. Quantitative analysis of P-Thr286 CaMKII in cytosol is shown on the right panel. Densitometric values of P-Thr 286 CaMKII are normalized for actin in the same samples. (**B**) Western blot analysis of HDAC7 in cytosolic fractions from diaphragm muscles and nuclear fractions from WT and C3KO quadriceps. Nuclei were fractionated from pooled muscles isolated from three mice for each genotype. The nuclear protein lamin B was used as a loading control and nuclear protein marker. Quantitative analyses of the blots are shown on the lower panels. For all graphs, vertical bars represent standard error.

Thus, CaMKII-mediated signaling was specifically blunted in C3KO muscles, resulting in a decrease in total and activated CaMKII and accumulation of a class II HDAC in the nuclear fraction.

Decreased expression of slow phenotype-associated genes in C3KO mice

Class II HDACs repress the activity of MEF2, a key transcriptional regulator of muscle development and adaptation that is responsive to Ca^{2+}-mediated signaling. MEF2 preferentially activates the slow muscle program and thus, decreased MEF2 activity is predicted to lead to reduced expression of slow versus fast phenotype-associated genes (16). To investigate whether this is the case in C3KO mice, we compared the transcriptomes of the soleus versus the quadriceps muscles in C3KO and WT mice. The soleus muscle has the highest representation of slow fibers (~30–50% slow fibers) of all mouse muscles, whereas the quadriceps is comprised of only fast fibers. Since skeletal muscle phenotype is modulated by functional demands, we used a within-animal comparison to diminish changes that might result from differences in physical activity in a given animal. In this comparison, we identified several slow phenotype-associated genes that were expressed at much lower levels in C3KO solei versus quadriceps compared with WT solei versus quadriceps. The expression of each of the identified genes was verified by quantitative real-time PCR (Fig. 4A and Supplementary Material, Fig. S1). For example, in WT mice, the expression of the *Myh7* gene encoding myosin heavy chain beta (MyHC-β) slow-twitch isoform was 986 times higher in solei than in quadriceps, whereas in C3KO mice this difference was only 219 times. Other affected genes included *Tnnt1* encoding slow skeletal muscle troponin T, *Tnnc1* encoding slow-twitch skeletal/cardiac muscle troponin C and *Tpm3* encoding slow muscle alpha-tropomyosin. Thus, the expression of slow-twitch isoforms of sarcomeric proteins was decreased in C3KO mice, consistent with reduced CaMK signaling and reduced MEF2 activity.

We also quantitated the representation of slow versus fast muscle fibers in solei of WT and C3KO mice by immunostaining with an antibody that specifically recognizes slow MyHC. This analysis revealed a significantly higher percentage of type I slow-twitch fibers in WT compared with C3KO solei (Fig. 4B). Thus, impaired CaMKII signaling in C3KO mice has a functional consequence of reduced expression of slow phenotype-associated genes and less representation of type I, slow-twitch fibers in the soleus.

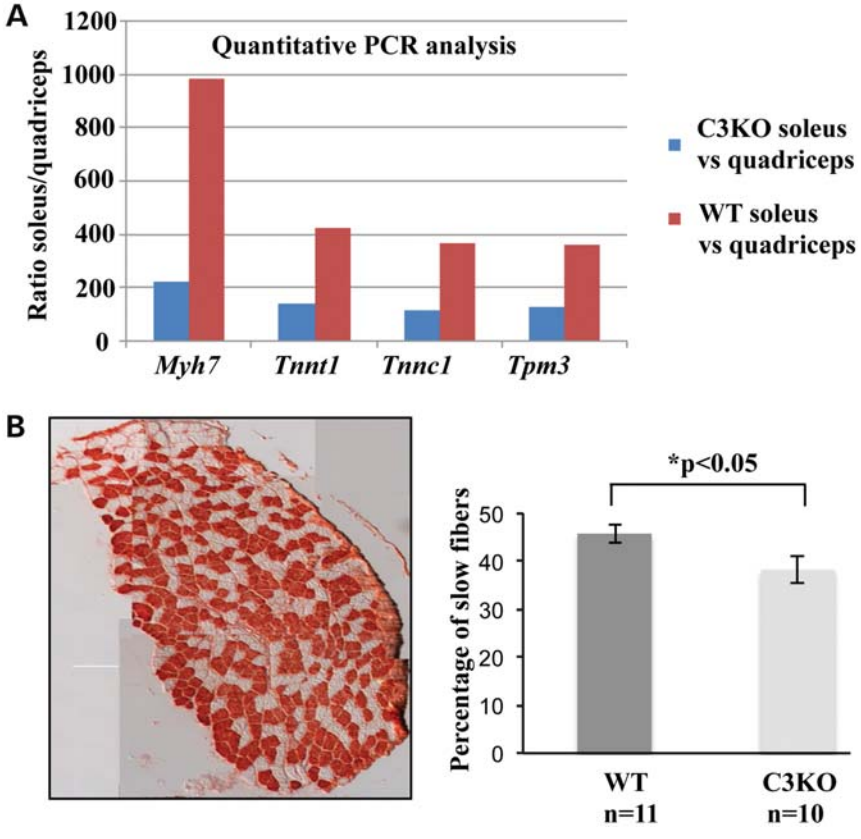

Figure 4. (**A**) Expression of slow phenotype-associated genes is decreased in C3KO mice. The fold change value of four different transcripts in the slow-twitch fiber-containing soleus, versus predominantly fast-twitch quadriceps muscles from the same animals. Comparisons were made in C3KO (soleus versus quadriceps) and WT (soleus versus quadriceps) muscles by quantitative real-time PCR. Transcripts analyzed: *Myh7*, MHC-β slow-twitch isoform gene; *Tnnt1*, slow skeletal muscle troponin T gene; *Tnnc1*, slow-twitch skeletal/cardiac muscle troponin C gene; *Tmp3*, slow muscle alpha-tropomyosin gene. (**B**) The percentage of slow fibers is decreased in C3KO solei. Quantitation is based on the analysis of mosaic images of the entire cross-sectional area of each soleus stained for slow MyHC (example of such image is shown on the left panel). Vertical bars represent standard error of the mean.

Adaptive response to physical activity is diminished in C3KO mice

Ca^{2+}-mediated signaling plays an important role in muscle's ability to adapt to changes in loading (15). Since signaling via CaMKII was significantly affected by the absence of CAPN3, we hypothesized that muscle adaptation to increased contractile activity would be diminished in C3KO mice. To validate this hypothesis, we subjected the mice to 3 weeks of increased physical activity by giving them access to running wheels (with wheel counters) in their cages (voluntary running exercise) and by subjecting them to forced running on a treadmill for 1 h every day, 5 days a week (non-voluntary running exercise). There was no significant difference between the amount of voluntary and treadmill running observed between C3KO and WT mice. As shown in Figure 5A, activated CaMKII was significantly increased in the WT plantaris muscle in response to this regimen; however, in the absence of CAPN3, the response was abolished. These changes were accompanied by a trend of increased expression of slow MyHC in WT muscles but not in C3KO muscles (Fig. 5B). These data demonstrate that the adaptive response to increased functional demand is compromised in C3KO muscles.

CAPN3 plays a structural role in maintaining the RyR complex in human muscle as it does in C3KO mice

Since we previously observed a reduction in RyR levels and decreased Ca^{2+} release upon activation in C3KO mice, we sought to determine whether similar changes could be observed in biopsies from patients with LGMD2A (Fig. 6). One biopsy was from a patient carrying a homozygous nonsense mutation 2069-2070delAC (patient 1, 18 years old) and two were from heterozygous patients carrying one nonsense and one missense mutation, leading to the amino acid substitutions K254E (patient 2, 27 years old) and R489W (patient 3, 48 years old). Histological analysis of these biopsies, especially from the younger patients, showed that, overall, the muscles were well-preserved with occasional small foci of degeneration and inflammation, and very few regenerating fibers expressing developmental myosin heavy chain (dMyHC). As was previously reported for LGMD2A, these biopsies also showed a high degree of fiber size variability with some extremely atrophic fibers, especially in patient 3 (Supplementary Material, Fig. S2). Although patient 1 is predicted to lack CAPN3 due to the nature of his mutation, patients 2 and 3 carry one allele of the *CAPN3* gene that could produce a mutant CAPN3 with just one amino acid substitution. Both of these substitutions were localized far away

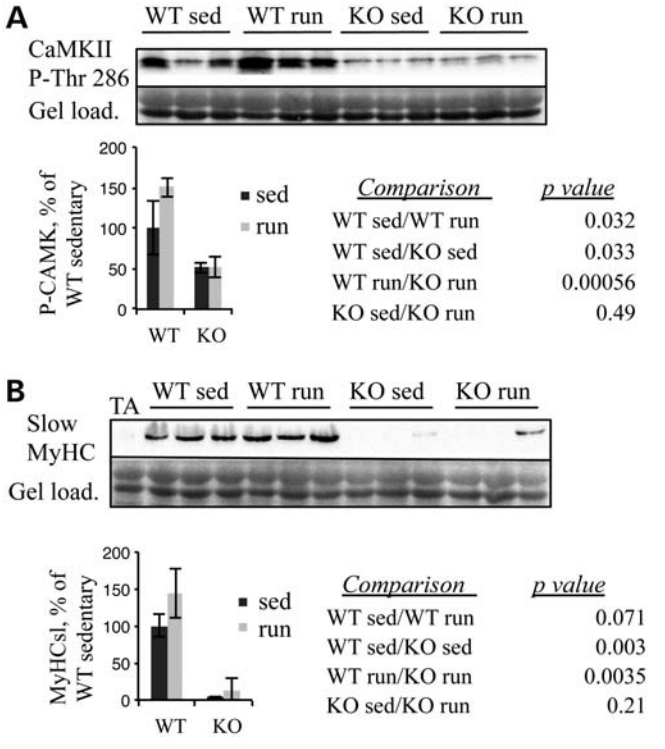

Figure 5. C3KO mice do not induce CaMKII pathway signaling in response to exercise training. (**A**) Western blot of whole-muscle extracts probed for the activated form of CaMKII. WT plantaris muscles increase CaMK activation in response to exercise training, whereas C3KO muscles do not demonstrate any elevation of CaMK. Quantitative and statistical analyses of the blot are shown below the blot. Vertical bars represent standard error of the mean. (**B**) Western blot of plantaris muscle extracts probed for slow MyHC (MyHCI). Although a trend of increased expression can be observed in WT muscles, expression of slow MyHC is decreased in C3KO mice and no elevation is observed in response to the exercise training. An extract from the TA (tibialis anterior, exclusively fast-twitch muscle) was used as a control for antibody specificity. Quantitative and statistical analyses of the blot are shown below the blot. Vertical bars represent standard error of the mean.

from the catalytic site in the predicted structural model of CAPN3 (Fig. 6A) and are not likely to affect proteolytic activity [a model was generated by protein structure homology modeling using SWISS-MODEL workspace and visualized by the PyMol software (17)]. To confirm this prediction, we introduced these mutations in CAPN3 and expressed the mutant proteins in insect cells to test their ability to autolyze *in vitro*. This test is based on the ability of proteolytically active CAPN3 to perform autolytic cleavage at strictly defined sites within the IS1 region, to produce an ~55 kDa fragment. Using the proteolytically inactive C129S mutant of CAPN3 as a negative control, we showed that both K254E and R489W mutants are active and produce the same 55 kDa autolytic fragment as a WT CAPN3 expressed under the same conditions (Fig. 6B). Thus, both missense mutations found in patients 2 and 3 do not affect the proteolytic activity of CAPN3.

We next examined levels of CAPN3 and RyR in these biopsies in comparison with a healthy control. Figure 6C shows that, as predicted, patient 1 lacked CAPN3, whereas both patients 2 and 3 had intermediate levels of CAPN3 compared with healthy controls. Levels of RyR were decreased in all three patients; moreover, RyR levels directly correlated with the level of CAPN3 (Fig. 6C and D). Similar results were obtained with two more LGMD2A biopsies and additional healthy biopsies and are presented in Supplementary Material, Figure S3. These data, together with mutant CAPN3 activity studies, lend further support for a structural role for CAPN3 in maintaining RyR at the triad, since reductions of CAPN3 in LGMD2A patients correlate with a proportional loss of RyR, similar to that observed in C3KO mice.

Decreased concentrations of RyR have been reported in multiminicore disease, a congenital myopathy caused by recessive mutations in the gene encoding *RyR1* (18,19). Multiminicores are histological manifestations of disorganized sarcomeres in which there is a deficiency of mitochondria and oxidative enzymes that can be revealed by staining for succinate dehydrogenase (SDH) activity (20). Staining of LGMD2A biopsies for SDH activity also revealed abnormalities similar to multiminicores, which became more prominent in patient 3 (Fig. 7A–D).

The data above demonstrate that LGMD2A muscle biopsies, similar to C3KO muscles, showed decreased levels of the major Ca^{2+} release channel RyR, leading to the hypothesis that they might also have impaired Ca^{2+} release and Ca^{2+}-mediated signaling. We performed western blot analysis of Ca^{2+}-mediated signaling components (CaMKII and Cn) in human muscle biopsies (data not shown), but results were inconclusive. Given the fact that the rare biopsy material we obtained was derived from different muscle groups and from patients of varying ages, it is likely that too many variables were present in these diverse biopsies to accurately assess CaMK signaling. Thus, it is not surprising that comparisons between biopsies collected from different muscles of patients and control subjects at different ages and different stages of disease progression are inconclusive. However, since CaMK signaling is especially important for maintaining slow fiber phenotype, we examined slow myofibers in LGMD2A biopsies by immunostaining human biopsies for slow MyHC. This analysis revealed that in all three LGMD2A patients, the most atrophic and abnormal fibers were slow-twitch type I fibers (Fig. 7E–H). These observations suggest that the ability to maintain a slow phenotype may be necessary for the health of slow myofibers and suggest that similar pathogenic mechanisms may operate in C3KO mice and LGMD2A patients.

DISCUSSION

In the current studies, we expanded upon our previous results that revealed an unexpected structural role for CAPN3 in the triad-associated protein complex (8). In the absence of CAPN3, several components of the triads, including the Ca^{2+}-releasing channel RyR, are reduced, and Ca^{2+} release upon activation is impaired. Here, we show that one downstream signaling pathway operating through Ca^{2+}-calmodulin and CaMKII is compromised in C3KO muscles, by demonstrating a significant reduction in the levels of total and activated CaMKII in C3KO muscle. These changes are specific for CaMK since levels of Cn, a key mediator of an alternative Ca^{2+} signaling pathway, were not decreased in the same muscles. We also observed the expected functional outcome

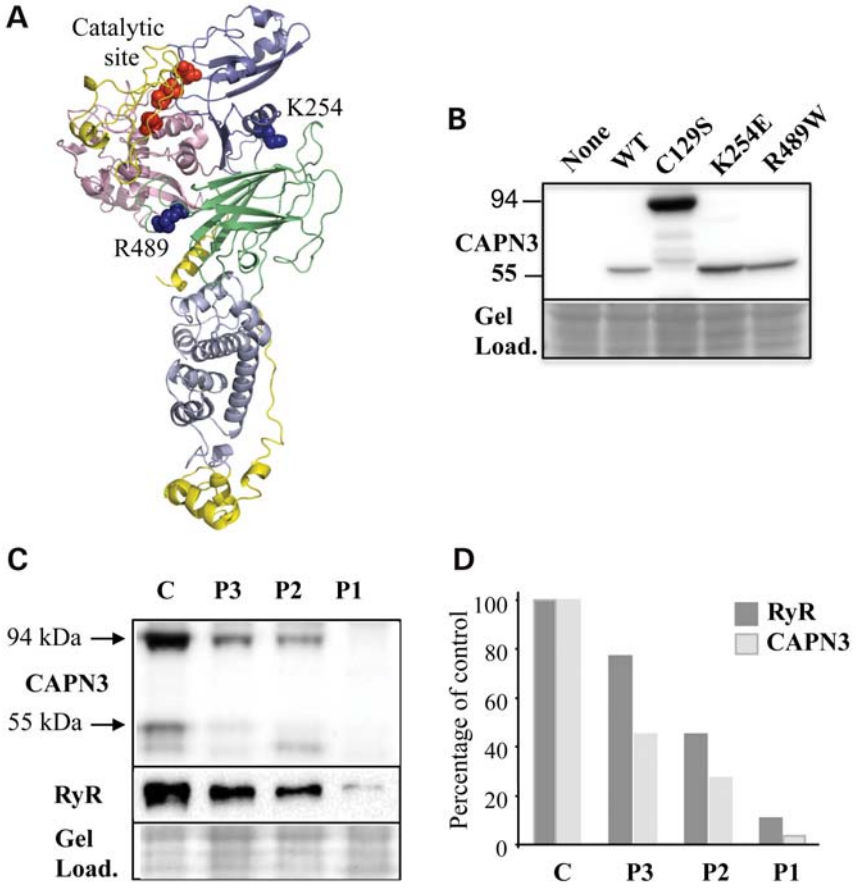

Figure 6. CAPN3 pathogenic mutations, K254E and R489W, do not affect proteolytic activity, but rather result in decreased CAPN3 and RyR levels in LGMD2A patient biopsies. (**A**) CAPN3 structure generated by protein structure homology modeling using SWISS-MODEL workspace shows that both mutations (shown in blue) are located far away from the active site (shown in red). (**B**) Western blot analysis of insect cells expressing either WT or mutant CAPN3. Autolytic activity of CAPN3 was used to test for CAPN3 proteolytic properties. Active CAPN3 undergoes autolysis and produces a 55 kDa fragment, whereas the proteolytically inactive C129S mutant is detected as the full-length 94 kDa protein. Both K254E and R489W mutant CAPN3s undergo autolysis in a manner that is indistinguishable from WT CAPN3. (**C**) Western blot analysis of CAPN3 and RyR expression in human muscle biopsy extracts shows decreased levels of both CAPN3 and RyR in LGMD2A patients (C, healthy subject; P1, P2, P3, three LGMD2A patients studied). (**D**) Quantitative analysis of CAPN3 and RyR immunoblots demonstrate a direct correlation between CAPN3 and RyR levels.

from the impaired CaMKII signaling, a reduction in expression of slow phenotype-associated genes in C3KO soleus versus quadriceps when compared with WT, accompanied by a decrease in the percentage of type I (slow-twitch) fibers in C3KO soleus muscles.

The two main skeletal muscle fiber types, slow twitch or type I and fast twitch or type II, differ significantly with respect to their contractile properties, metabolism and pattern of gene expression. Slow-twitch myofibers exhibit increased oxidative metabolism, more abundant mitochondria and resistance to fatigue, which can enhance overall muscle endurance (21). Previously, we found that mitochondria are abnormal and ATP production is decreased in C3KO muscles compared with age- and gender-matched WT muscles, a result that is consistent with compromised oxidative metabolism (22). Since oxidative metabolism is a significant feature of slow-twitch fibers, these data also support a functional consequence of an impaired slow phenotype in C3KO mice. Interestingly, soleus and diaphragm muscles are the most affected muscles in the C3KO mouse model. Our current data provide a possible explanation for the selective involvement of these muscles, since soleus and diaphragm muscles are rare in that they possess a significant proportion of slow-twitch fibers. These muscles are most similar to human skeletal muscles, which are of mixed muscle phenotypes (23).

Functional overload and exercise training result in an increased proportion of slow fibers in the muscle, whereas decreased contractile activity due to immobility or disease leads to a slow-to-fast phenotypic conversion (24). This plasticity plays a key role in muscle's ability to adapt to changes in functional demand. An inability of muscle to meet the functional requirements can result in muscle failure. Several signaling pathways, including CaMKII pathway, have been implicated in these adaptive responses (13). It was shown that CaMK II activity was increased in muscles following 7 days of stretch overload or 2 weeks of voluntary wheel running (25). We also found that when WT mice were subjected to exercise training, the CaMKII signaling pathway was activated, leading to increased expression of slow

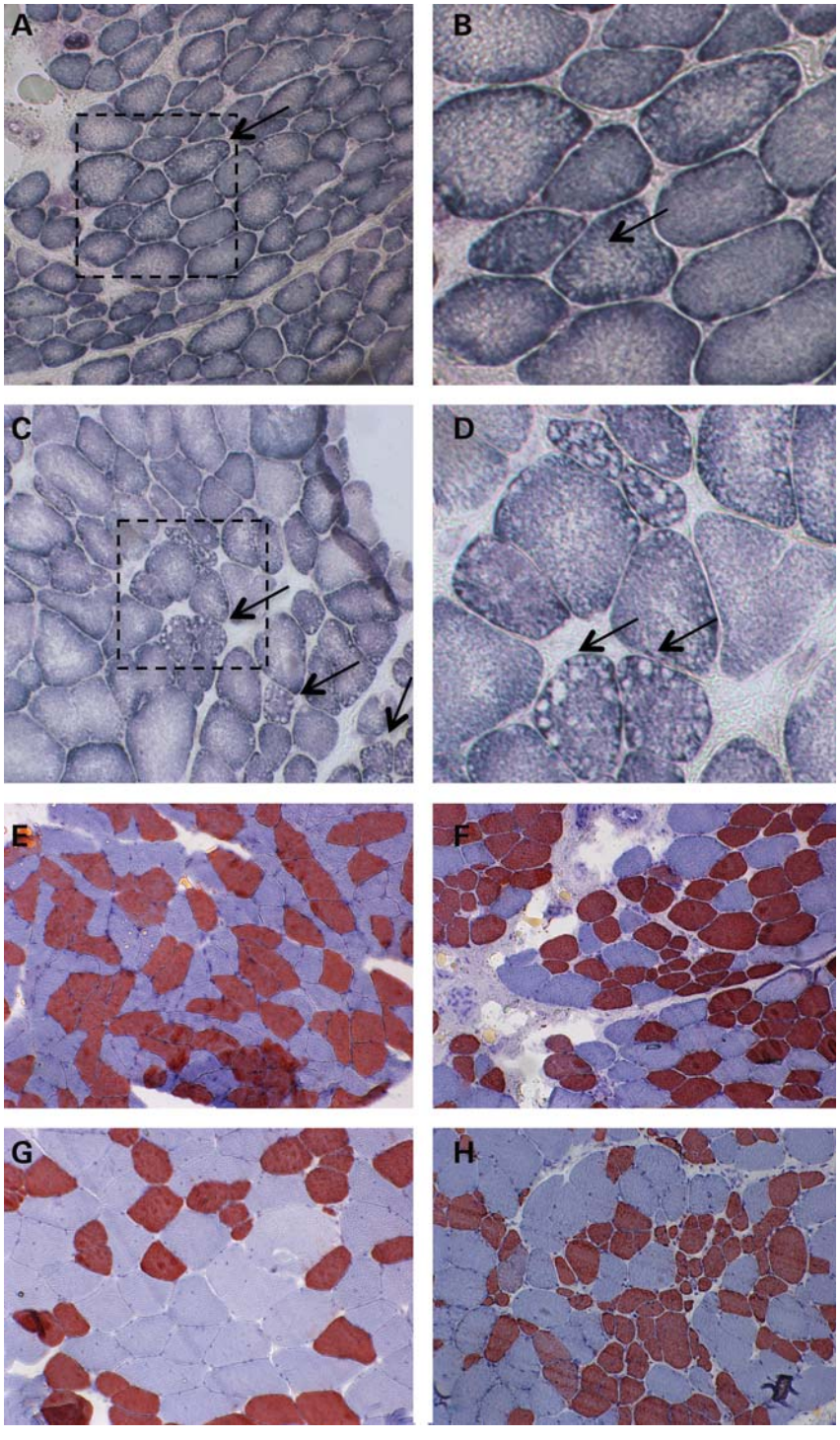

Figure 7. Affected fibers in LGMD2A biopsies are primarily slow and contain multiminicores. (**A**–**D**) Histochemical staining of LGMD2A muscle biopsies for SDH reveals multiple foci of disorganized sarcomeres that lack mitochondria. The biopsy from patient 1 (18 years old) (A and B) has fewer abnormal fibers compared with the patient 3 (48 years) (C and D). (B) and (D) Magnified areas identified on (A) and (C), respectively. Arrows point to some of the abnormal fibers. (**E**–**H**) Muscle biopsies from a healthy subject (E) or LGMD2A patients 1 (F), 2 (G) and 3 (H) stained for slow MyHC. Most of the small-diameter fibers are stained positive for slow MyHC (red). Slides are counterstained with aqueous hematoxylin (blue).

MyHC in the plantaris muscle, which normally has a very low percentage of slow-twitch fibers. Unlike WT mice, C3KO mice did not respond to exercise training in the same manner as WT, strongly suggesting that the adaptation response is compromised in muscles lacking CAPN3.

CaMKII is composed of two sets of six subunits that form stacked, hexagonally shaped rings (26). Each subunit contains an N-terminal catalytic domain and a C-terminal association domain. The initial step of CaMKII activation requires its association with Ca^{2+}/calmodulin and results in

Table 1. LGMD2A patients' clinical information

Patients	Age at the time of biopsy	Age at onset	Sex	Mutation	GMW Scale[a]	Evolution index[b]	Wheel-chair bound
P1	19	12	M	2069-70delAC (homozygous)	V	5/7 = 0.71	No
P2	29	15	M	K254E/1910delC	II	2/14 = 0.14	No
P3	49	20	F	R489W/c.2362_2363 delinsTCATCT	VII	7/29 = 0.24	Yes

[a]Based on Gardner-Medwin and Walton (42).
[b]Evolution index: GMW scale number divided by years of evolution.

autophosphorylation. Once phosphorylated, CaMKII becomes constitutively active (i.e. Ca^{2+}/calmodulin-independent), thus allowing kinase activity to continue even after Ca^{2+} concentration is decreased. Prolonged durations of Ca^{2+} pulses lead to larger numbers of activated and autophosphorylated CaMKII subunits, thus producing higher levels of autonomous activity (15,27) that will persist even after a bout of contractile activity. This unique mechanism is thought to be responsible for the long-lasting effect of CaMKII pathway activation on downstream processes. Besides a role for CaMKII in the maintenance of myofiber phenotype, some data also point to a role in muscle growth (25). We found that C3KO muscles are atrophic and they fail to grow after disuse-induced atrophy (28). However, whether or not the lack of CaMKII activation is responsible for these abnormalities remains to be studied. Finally, CaMKII was recently shown to be a key regulator of contraction-induced glucose uptake. Overexpression of a CaMKII-specific inhibitory peptide caused a significant decrease in contraction-induced but not insulin-induced glucose uptake (29). These findings suggest that energy deficit may also play a role in pathogenic changes due to decreased activation of CaMKII. Thus, CaMKII signaling insufficiency may have multiple and divergent effects on muscle function, including the maintenance of slow fiber phenotype, control of energy metabolism and the adaptive response to changes in muscle loading.

Consistent with our studies using the C3KO mouse model, biopsies from LGMD2A patients also showed decreased RyR; moreover, the level of RyR directly correlated with the level of CAPN3 in these patient biopsies. Importantly, no correlation was observed between the extent of histopathological changes in patients' biopsies and levels of RyR. The muscle biopsy from the youngest patient carrying a homozygous frame shift mutation (patient 1) showed no detectable CAPN3 and the lowest RyR, whereas histological examination of this biopsy revealed very well-preserved tissue with minimal changes compared with the patient 3 with the highest content of both CAPN3 and RyR, but with disease at a much more advanced stage. These observations strongly suggest that changes in RyR levels are not non-specific consequences of pathological muscle degeneration but rather a primary defect that directly correlates with CAPN3 mutations. Moreover, as shown in Table 1, patient 1 (who is the youngest but has the lowest level of RyR) has the most severe disease progression as reflected by evolution index (0.71). These data showed that there is a direct correlation between the level of CAPN3 and RyR, and the severity of the disease, suggesting that a reduction in RyR may be an important contributing factor to the pathogenic pathway and it is not a non-specific consequence of increased tissue degeneration.

Since similar changes in RyR content led to significant decreases in Ca^{2+} release upon excitation in C3KO muscles, it seems reasonable to assume that Ca^{2+} transport is also affected in LGMD2A patients, even though we did not have an opportunity to directly measure Ca^{2+} release in the patients. Unlike in mice, human muscles comprise a mix of slow-twitch and fast-twitch fibers. Genetic factors as well as the type and level of physical activity carried out by the patient may determine their relative expression. These variances make direct comparisons of the fiber-type proportion between LGMD2A patients and healthy subjects difficult. However, we found that slow-twitch fibers in LGMD2A patients studied are preferentially atrophic and disorganized, suggesting that the ability to maintain the integrity and health of slow-twitch fibers is compromised in LGMD2A patients. Similar observations were also reported in studies of Reunion Island and Japanese LGMD2A patients (30,31).

Several lines of evidence suggest that expression of the slow-twitch program is beneficial for dystrophic muscle, at least in the mouse model for Duchenne muscular dystrophy (mdx mouse). It was shown that targeted inhibition of Ca^{2+}/CaM-dependent signaling by overexpression of CaM-binding protein driven by the slow fiber-specific troponin I promoter exacerbates the dystrophic phenotype (32). These pathological changes were associated with a predicted decrease in the transcription of the slow phenotype genes such as *MyHCI* (slow) and the transcription factor *PGC-1*α (peroxisome proliferator γ co-activator 1α). PGC-1α was shown to regulate adaptive mitochondrial function in many tissues, including skeletal muscle (33). In muscle, PGC-1α expression is controlled by the activity of both Cn and CaMK type IV and regulates mitochondrial biogenesis and expression of neuromuscular junction proteins (34). Transgenic expression of PGC-1α in skeletal muscles of the mdx mice ameliorates muscular dystrophy and improves a number of parameters including muscle histology and running performance (35). Whether expression of slow program genes is beneficial for other types of muscular dystrophies remains to be determined, but at least for the Duchenne muscular dystrophy model, perturbations of Ca^{2+}-mediated signaling greatly worsen disease severity.

In summary, data presented here and our previous studies (8) suggest a novel pathogenic mechanism never before described for any muscular dystrophy that includes decreased Ca^{2+} release upon excitation, blunted Ca^{2+}-mediated signaling and lack of an adequate adaptive response to increased muscle activity. These studies also expose one potential underlying pathogenic mechanism in LGMD2A and identify the

CaMKII-mediated pathway as a potential target that should be tested for pharmacological intervention. Given the fact that CAPN3 has been implicated in diverse processes in muscle, the relationship between CAPN3, CaMKII and other possible pathological mechanisms remains to be determined.

MATERIALS AND METHODS

Muscle extract fractionation and western blotting

For western blot analysis of total muscle extracts, muscles were homogenized in a Dounce homogenizer in reducing sample buffer (80 mM Tris, pH 6.8, 0.1 M dithiothreitol, 2% SDS and 10% glycerol) with protease inhibitors cocktail (Sigma). For isolation of cytosolic and membrane fractions, muscles were homogenized in detergent-free buffer (0.2 mM EDTA, 0.25 M sucrose and 10 mM Tris–HCl, pH 7.8) with protease inhibitors cocktail (Sigma) and subjected to a series of centrifugations at 2000*g* for 8 min, 12 000*g* for 15 min and 130 000*g* for 60 min at 4°C. The first two centrifugations removed myofibrils, nuclei and mitochondria. After the last centrifugation, the supernatant contained cytosolic proteins, whereas the pellet was enriched in membranes.

Nuclei were isolated using Percoll density centrifugation as described (36). Briefly, muscles were homogenized in a homogenization buffer (15 mM Hepes, pH 7.5, 0.3 M sucrose, 60 mM KCl, 0.15 mM spermine, 0.5 mM spermidine, 14 mM β-mercaptoethanol, 10 mg/ml BSA) with 0.5 mM EGTA, 2 mM EDTA and centrifuged at 2000*g* for 5 min. Pellets were homogenized in the same buffer with 0.1 mM EGTA and 0.1 mM EDTA and 0.5% Triton X-100 and filtered through a nylon mesh before adding Percoll to a final concentration of 27% (v/v). Homogenate was added to a tube containing Percoll (approximately one-third of the homogenate volume), mixed and centrifuged at 27 000*g* for 15 min. Nuclei formed a layer near the bottom of the tube that was carefully removed with a sialinized Pasteur pipette, washed and collected by centrifugation. Nuclear proteins were extracted using Trizol (Invitrogen) as described (37). The following antibodies were used for western blot analyses: anti-CaMKIIb (Zymed), anti-pan-Cn (Cell Signaling), anti-P-Thr286 CaMKII (Thermo), anti-HDAC7 (Cell Signaling), anti-lamin B (Zymed), anti-slow MyHC (Novocastra), anti-calpain 3 12A2, raised against a synthetic peptide containing amino acids 355–370 of the human CAPN3 sequence (Novocastra). Anti-calpain 3 IS2 antibody (raised against a synthetic peptide containing amino acids 586–605) was a generous gift from Dr H. Sorimachi.

Mice exercise protocol

For voluntary wheel-running exercise, mice were housed in running cages for the whole duration of the experiment (4 weeks). During the first week, mice were accustomed to the treadmill (Columbus Instruments) with a 15 min run once per day at 10 m/min. For the next 3 weeks, mice were subjected to forced running exercise performed on a 10% incline at 10 m/min for the first 20 min followed by 40 min at 15 m/min. At the end of 4 weeks, mice were sacrificed and soleus, plantaris and tibialis anterior muscles were collected for analyses. All mice used for this experiment were males, aged 3.5–4 months by the end of the experiment. All experimental protocols conducted and the use of animals were in accordance with the National Institute of Health Guide for Care and Use of Laboratory Animals and approved by the UCLA Institutional Animal Care and Use Committee.

In vitro mutagenesis and expression of mutant CAPN3s in insect cells

CAPN3 mutants (C129S, K354E and R489W) were generated in the full-length WT C3 cDNA in pGEX2T, using the QuikChange II Site-Directed Mutagenesis Kit (Stratagene). The following primers were used to introduce mutations—C129S: 5′ GGAGATCTAGGGGACAGCTGGTTTCTTGCA GCC and 5′ GGCTGCAAGAAACCAGCTGTCCCCTAGAT CTCC; K254E: 5′ GTACAAGATTATGAGGGAAGCTATC GAGAGAGGC and 5′ GCCTCTCTCGATAGCTTCCCTCA TAATCTTGTAC; R489W: 5′ CTGATGCAGAAGAACTGG CGCAAGGACCGGAAG and 5′ CTTCCGGTCCTTGCGCC AGTTCTTCTGCATCAG.

To test for CAPN3 autolytic activity, WT CAPN3, the proteolytically inactive CAPN3 mutant C129S or other mutant CAPN3s (K354E and R489W) were expressed in a baculovirus system according to the manufacturer's recommendations (BD Biosciences) as was described previously (38). Briefly, insect cells were plated at 50–70% confluence and infected with various CAPN3 constructs, using high-titer viral stocks. After 3 days, cells were collected and analyzed by western blot, using the anti-CAPN3 12A2 antibody, which detects both the full-length form (94 kDa) and autolytically produced fragments (~55 kDa).

Microarray analysis and RT-PCR

Soleus and quadriceps muscles were collected from 11 WT and 11 C3KO males. The microarray experiment was performed according to the manufacturers' instructions as was described previously (39). Briefly, cDNA was generated from RNA samples, and biotinylated cRNA was transcribed *in vitro*. Fragmented cRNA was hybridized with GeneChip-MouseGenome 430 2.0 microarrays (Affymetrix, Santa Clara, CA, USA). These microarrays analyze the expression of over 39 000 transcripts and variants from over 34 000 well-characterized mouse genes, using 45 000 probes. The hybridized arrays were scanned, and raw data were extracted using the Microarray Analysis Suite 5.0 (MAS5; Affymetrix). To identify significantly different gene expression, a geometric fold-change analysis was used (40,41). The threshold was set at a two-fold change value. Class comparison difference analyses were performed using BRB-Array Tools developed by Dr Richard Simon and the BRB-Array Tools Development Team.

To validate array data, expression levels of the differentially expressed genes were measured by the TaqMan quantitative RT-PCR, using the 7900 HT Fast Real-Time PCR System (Applied Biosystems). The TaqMan Low Density Arrays (TLDAs) and the TaqMan probes were purchased from Applied Biosystems. Expression levels for all transcripts in

the TLDAs were determined relative to the internal housekeeping control gene 18S.

LGMD2A patients

For diagnostic purposes, deltoid, quadriceps or biceps muscle specimens were collected from five LGMD2A patients, using institutionally approved protocols in the Hospital Universitario Donostia, Spain. Samples were de-identified and sent to the Spencer Lab. The patients were both males and females, ages from 19 to 49, and with the age at the onset from 12 to 20. Three patients were studied in more detail (Table 1), including histochemical staining for NADH and SDH and immunostaining using anti-slow MyHC antibody (Novocastra). The biopsies were taken from the following muscles: patient 1, no information; patient 2, deltoid; patient 3 and control subject, quadriceps. Clinical information about these patients is presented in Table 1.

SUPPLEMENTARY MATERIAL

Supplementary Material is available at *HMG* online.

Conflict of Interest statement. None declared.

FUNDING

This work was supported by grants from the National Institute of Arthritis, Musculoskeletal and Skin Diseases (RO1 AR052693, RO1 AR/NS48177), and a P30 Muscular Dystrophy Core Center (P30AR057230-01) awarded from the National Institutes of Arthritis, Musculoskeletal and Skin Diseases. This work was also funded by the Muscular Dystrophy Association and the Crystal Ball for a Cure Inc. This work was also supported by grants from the Health Research Fund (FIS: PI010-00848, PS09-00660) of the Spanish Ministry of Science and Innovation; the European Union (ERDF); and the Department of Health of the Government of the Basque Country (2009111025); as well as grants awarded to authors O.J. by the Basque Government (AE-BFI-08.164) and A.S. by the Spanish Ministry of Health (FIS: CP06/00099); and support from the Basque Foundation for Health Innovation and Research (BIOEF) promoted by the Basque Government Department of Health.

REFERENCES

1. Richard, I., Broux, O., Allamand, V., Fougerousse, F., Chiannilkulchai, N., Bourg, N., Brenguier, L., Devaud, C., Pasturaud, P., Roudaut, C. *et al.* (1995) Mutations in the proteolytic enzyme calpain 3 cause limb-girdle muscular dystrophy type 2A. *Cell*, **81**, 27–40.
2. Sorimachi, H., Hata, S. and Ono, Y. (2010) Expanding members and roles of the calpain superfamily and their genetically modified animals. *Exp. Anim.*, **59**, 549–566.
3. Kramerova, I., Beckmann, J.S. and Spencer, M.J. (2007) Molecular and cellular basis of calpainopathy (limb girdle muscular dystrophy type 2A). *Biochim. Biophys. Acta*, **1772**, 128–144.
4. Milic, A., Daniele, N., Lochmuller, H., Mora, M., Comi, G.P., Moggio, M., Noulet, F., Walter, M.C., Morandi, L., Poupiot, J. *et al.* (2007) A third of LGMD2A biopsies have normal calpain 3 proteolytic activity as determined by an in vitro assay. *Neuromuscul. Disord.*, **17**, 148–156.
5. Goll, D.E., Thompson, V.F., Li, H., Wei, W. and Cong, J. (2003) The calpain system. *Physiol. Rev.*, **83**, 731–801.
6. Diaz, B.G., Moldoveanu, T., Kuiper, M.J., Campbell, R.L. and Davies, P.L. (2004) Insertion sequence 1 of muscle-specific calpain, p94, acts as an internal propeptide. *J. Biol. Chem.*, **279**, 27656–27666.
7. Taveau, M., Bourg, N., Sillon, G., Roudaut, C., Bartoli, M. and Richard, I. (2003) Calpain 3 is activated through autolysis within the active site and lyses sarcomeric and sarcolemmal components. *Mol. Cell Biol.*, **23**, 9127–9135.
8. Kramerova, I., Kudryashova, E., Wu, B., Ottenheijm, C., Granzier, H. and Spencer, M.J. (2008) Novel role of calpain-3 in the triad-associated protein complex regulating calcium release in skeletal muscle. *Hum. Mol. Genet.*, **17**, 3271–3280.
9. Franzini-Armstrong, C. (1994) The sarcoplasmic reticulum and the transverse tubules. In Engel, A.G. and Franzini-Armstrong, C. (eds), *Myology*. McGraw-Hill, Inc., New York, Vol. 1, pp. 176–199.
10. Dayanithi, G., Richard, I., Viero, C., Mazuc, E., Mallie, S., Valmier, J., Bourg, N., Herasse, M., Marty, I., Lefranc, G. *et al.* (2009) Alteration of sarcoplasmic reticulum Ca release in skeletal muscle from calpain 3-deficient mice. *Int. J. Cell Biol.*, **2009**, 340346.
11. Ojima, K., Ono, Y., Ottenheijm, C., Hata, S., Suzuki, H., Granzier, H. and Sorimachi, H. (2011) Non-proteolytic functions of calpain-3 in sarcoplasmic reticulum in skeletal muscles. *J. Mol. Biol.*, **407**, 439–449.
12. Chin, E.R. (2004) The role of calcium and calcium/calmodulin-dependent kinases in skeletal muscle plasticity and mitochondrial biogenesis. *Proc. Nutr. Soc.*, **63**, 279–286.
13. Bassel-Duby, R. and Olson, E.N. (2006) Signaling pathways in skeletal muscle remodeling. *Ann. Rev. Biochem.*, **75**, 19–37.
14. Fong, Y.L., Taylor, W.L., Means, A.R. and Soderling, T.R. (1989) Studies of the regulatory mechanism of Ca2+/calmodulin-dependent protein kinase II. Mutation of threonine 286 to alanine and aspartate. *J. Biol. Chem.*, **264**, 16759–16763.
15. Chin, E.R. (2005) Role of Ca2+/calmodulin-dependent kinases in skeletal muscle plasticity. *J. Appl. Physiol.*, **99**, 414–423.
16. Potthoff, M.J., Wu, H., Arnold, M.A., Shelton, J.M., Backs, J., McAnally, J., Richardson, J.A., Bassel-Duby, R. and Olson, E.N. (2007) Histone deacetylase degradation and MEF2 activation promote the formation of slow-twitch myofibers. *J. Clin. Invest.*, **117**, 2459–2467.
17. Ermolova, N., Kudryashova, E., DiFranco, M., Vergara, J., Kramerova, I. and Spencer, M.J. (2011) Pathogenity of some limb girdle muscular dystrophy mutations can result from reduced anchorage to myofibrils and altered stability of calpain 3. *Hum. Mol. Genet.*, **20**, 3331–3345.
18. Zorzato, F., Jungbluth, H., Zhou, H., Muntoni, F. and Treves, S. (2007) Functional effects of mutations identified in patients with multiminicore disease. *IUBMB Life*, **59**, 14–20.
19. Zhou, H., Jungbluth, H., Sewry, C.A., Feng, L., Bertini, E., Bushby, K., Straub, V., Roper, H., Rose, M.R., Brockington, M. *et al.* (2007) Molecular mechanisms and phenotypic variation in RYR1-related congenital myopathies. *Brain*, **130**, 2024–2036.
20. Dubowitz, V. and Sewry, C.A. (2007) *Muscle Biopsy: A Practical Approach*. Sanders/Elsevier, Edinburgh.
21. Sugiura, T., Miyata, H., Kawai, Y., Matoba, H. and Murakami, N. (1993) Changes in myosin heavy chain isoform expression of overloaded rat skeletal muscles. *Int. J. Biochem.*, **25**, 1609–1613.
22. Kramerova, I., Kudryashova, E., Wu, B., Germain, S., Vandenborne, K., Romain, N., Haller, R., Verity, M.A. and Spencer, M.J. (2009) Mitochondrial abnormalities, energy deficit and oxidative stress are features of calpain 3 deficiency in skeletal muscle. *Hum. Mol. Genet.*, **18**, 3194–3205.
23. Kho, A.T., Kang, P.B., Kohane, I.S. and Kunkel, L.M. (2006) Transcriptome-scale similarities between mouse and human skeletal muscles with normal and myopathic phenotypes. *BMC Musculoskelet. Disord.*, **7**, 23–31.
24. Talmadge, R.J. (2000) Myosin heavy chain isoform expression following reduced neuromuscular activity: potential regulatory mechanisms. *Muscle Nerve*, **23**, 661–679.
25. Fluck, M., Waxham, M.N., Hamilton, M.T. and Booth, F.W. (2000) Skeletal muscle Ca(2+)-independent kinase activity increases during either hypertrophy or running. *J. Appl. Physiol.*, **88**, 352–358.
26. Kolodziej, S.J., Hudmon, A., Waxham, M.N. and Stoops, J.K. (2000) Three-dimensional reconstructions of calcium/calmodulin-dependent (CaM) kinase IIalpha and truncated CaM kinase IIalpha reveal a unique

organization for its structural core and functional domains. *J. Biol. Chem.*, **275**, 14354–14359.
27. Soderling, T.R., Chang, B. and Brickey, D. (2001) Cellular signaling through multifunctional Ca2+/calmodulin-dependent protein kinase II. *J. Biol. Chem.*, **276**, 3719–3722.
28. Kramerova, I., Kudryashova, E., Venkatraman, G. and Spencer, M.J. (2005) Calpain 3 participates in sarcomere remodeling by acting upstream of the ubiquitin-proteasome pathway. *Hum. Mol. Genet.*, **14**, 2125–2134.
29. Witczak, C.A., Jessen, N., Warro, D.M., Toyoda, T., Fujii, N., Anderson, M.E., Hirshman, M.F. and Goodyear, L.J. (2010) CaMKII regulates contraction- but not insulin-induced glucose uptake in mouse skeletal muscle. *Am. J. Physiol. Endocrinol. Metab.*, **298**, E1150–E1160.
30. Chae, J., Minami, N., Jin, Y., Nakagawa, M., Murayama, K., Igarashi, F. and Nonaka, I. (2001) Calpain 3 gene mutations: genetic and clinico-pathologic findings in limb-girdle muscular dystrophy. *Neuromus. Dis.*, **11**, 547–555.
31. Fardeau, M., Hillaire, D., Mignard, C., Feingold, N., Feingold, J., Mignard, D., de Ubeda, B., Collin, H., Tome, F.M., Richard, I. *et al.* (1996) Juvenile limb-girdle muscular dystrophy. Clinical, histopathological and genetic data from a small community living in the Reunion Island. *Brain*, **119**, 295–308.
32. Chakkalakal, J.V., Michel, S.A., Chin, E.R., Michel, R.N. and Jasmin, B.J. (2006) Targeted inhibition of Ca2+/calmodulin signaling exacerbates the dystrophic phenotype in mdx mouse muscle. *Hum. Mol. Genet.*, **15**, 1423–1435.
33. Handschin, C. and Spiegelman, B.M. (2006) Peroxisome proliferator-activated receptor gamma coactivator 1 coactivators, energy homeostasis, and metabolism. *Endocr. Rev.*, **27**, 728–735.
34. Handschin, C., Rhee, J., Lin, J., Tarr, P.T. and Spiegelman, B.M. (2003) An autoregulatory loop controls peroxisome proliferator-activated receptor gamma coactivator 1alpha expression in muscle. *Proc. Natl Acad. Sci. USA*, **100**, 7111–7116.
35. Handschin, C., Kobayashi, Y.M., Chin, S., Seale, P., Campbell, K.P. and Spiegelman, B.M. (2007) PGC-1alpha regulates the neuromuscular junction program and ameliorates Duchenne muscular dystrophy. *Genes Dev.*, **21**, 770–783.
36. Hahn, C.G. and Covault, J. (1990) Isolation of transcriptionally active nuclei from striated muscle using Percoll density gradients. *Anal. Biochem.*, **190**, 193–197.
37. Kirkland, P.A., Busby, J., Stevens, S. Jr. and Maupin-Furlow, J.A. (2006) Trizol-based method for sample preparation and isoelectric focusing of halophilic proteins. *Anal. Biochem.*, **351**, 254–259.
38. Kramerova, I., Kudryashova, E., Tidball, J.G. and Spencer, M.J. (2004) Null mutation of calpain 3 (p94) in mice causes abnormal sarcomere formation in vivo and in vitro. *Hum. Mol. Genet.*, **13**, 1373–1388.
39. Saenz, A., Azpitarte, M., Armananzas, R., Leturcq, F., Alzualde, A., Inza, I., Garcia-Bragado, F., De la Herran, G., Corcuera, J., Cabello, A. *et al.* (2008) Gene expression profiling in limb-girdle muscular dystrophy 2A. *PLoS One*, **3**, e3750.
40. Bakay, M., Zhao, P., Chen, J. and Hoffman, E.P. (2002) A web-accessible complete transcriptome of normal human and DMD muscle. *Neuromuscul. Disord.*, **12** (Suppl. 1), S125–S141.
41. Haslett, J.N., Sanoudou, D., Kho, A.T., Han, M., Bennett, R.R., Kohane, I.S., Beggs, A.H. and Kunkel, L.M. (2003) Gene expression profiling of Duchenne muscular dystrophy skeletal muscle. *Neurogenetics*, **4**, 163–171.
42. Gardner-Medwin, D. and Walton, J.N. (1974) The clinical examination of voluntary muscles. In Walton, J.N. (ed.), *Disorders of Voluntary Muscles*. Churchill Livingstone, Edinburgh, UK, pp. 517–560.